



# Calycosin Alleviates Sepsis-Induced Acute Lung Injury *via* the Inhibition of Mitochondrial ROS-Mediated Inflammasome Activation

Yu Xia<sup>1\*</sup>, Yuanbao Cao<sup>1</sup>, Yao Sun<sup>1</sup>, Xiuying Hong<sup>1</sup>, Yingyan Tang<sup>1</sup>, Juan Yu<sup>2</sup>, Hongjuan Hu<sup>3</sup>, Wenjia Ma<sup>1</sup>, Kailun Qin<sup>1</sup> and Rui Bao<sup>4</sup>

<sup>1</sup>Department of Pediatrics, LiShui People Hospital, Nanjing, China, <sup>2</sup>Department of Clinical Laboratory, LiShui People Hospital, Nanjing, China, <sup>3</sup>Department Science and Education, LiShui People Hospital, Nanjing, China, <sup>4</sup>Department of Pharmaceutics, School of Pharmacy of Jiangsu University, Zhenjiang, China

## OPEN ACCESS

### Edited by:

Jian Zhang,  
Tianjin Medical University, China

### Reviewed by:

Po-Jen Chen,  
Providence University, Taiwan  
Roman A. Zinovkin,  
Lomonosov Moscow State University,  
Russia

### \*Correspondence:

Yu Xia  
1367703936@qq.com

### Specialty section:

This article was submitted to  
Inflammation Pharmacology,  
a section of the journal  
Frontiers in Pharmacology

Received: 07 April 2021

Accepted: 14 September 2021

Published: 19 October 2021

### Citation:

Xia Y, Cao Y, Sun Y, Hong X, Tang Y,  
Yu J, Hu H, Ma W, Qin K and Bao R  
(2021) Calycosin Alleviates Sepsis-  
Induced Acute Lung Injury *via* the  
Inhibition of Mitochondrial ROS-  
Mediated Inflammasome Activation.  
*Front. Pharmacol.* 12:690549.  
doi: 10.3389/fphar.2021.690549

Sepsis-induced acute lung injury (ALI) culminates in multiple organ failure via uncontrolled inflammatory responses and requires effective treatment. Herein, we aimed to investigate the effect of calycosin (CA), a natural isoflavonoid, on sepsis-induced ALI. CA attenuated lipopolysaccharide (LPS) and cecal ligation and puncture (CLP)-induced structural damage and inflammatory cell infiltration in lung tissues by histopathological analysis. CA significantly reduced lung wet/dry ratio, inflammatory cell infiltration in bronchoalveolar lavage fluid, and myeloperoxidase activity. Moreover, CA improved the survival of septic mice. CA also substantially inhibited interleukin (IL)-1 $\beta$  and IL-18 levels and cleaved caspase 1 expression and activity in lung tissues. Additionally, CA markedly suppressed oxidative stress by increasing levels of superoxide dismutase and glutathione while decreasing malondialdehyde. *In vitro* assay showed that CA significantly inhibited LPS-induced IL-1 $\beta$  and IL-18 levels and cleaved caspase 1 expression and activity in BMDMs. Moreover, CA blocked the interaction among NLRP3, ASC, and caspase 1 in LPS-treated cells. CA markedly reduced mitochondrial ROS levels. Significantly, compared with CA treatment, the combination of CA and MitoTEMPO (mitochondria-targeted antioxidant) did not further reduce the IL-1 $\beta$  and IL-18 levels and cleaved caspase 1 expression and activity and decreased mitochondrial ROS levels. Collectively, the inhibition of mitochondrial ROS-mediated NLRP3 inflammasome activation contributes to the protective effects of CA, which may be considered a potential therapeutic agent for septic ALI.

**Keywords:** calycosin, sepsis, acute lung injury, inflammasome, reactive oxygen species

## INTRODUCTION

Sepsis remains a major problem for human health worldwide. The third international consensus definition for sepsis and septic shock defined sepsis as a “life-threatening dysfunction of organ induced by dysregulation of host response to infection” (Singer et al., 2016). Roughly 1 million Americans have been reported to suffer from sepsis annually, with about a 40% mortality rate (Aziz et al., 2013; Vincent et al., 2014). The cause of septic-induced pathophysiological abnormalities

involves the unrestrained reaction of the immune system (“cytokine storm”) to micro-organisms and their products (Hotchkiss and Karl, 2003).

Acute lung injury (ALI) and its severe form, acute respiratory distress syndrome (ARDS), are major health conditions that aggravate the mortality and morbidity of sepsis globally (Aziz et al., 2018). The susceptibility of lungs to injury manifests during sepsis, with over 50% of septic patients developing ALI or ARDS (Sevransky et al., 2009; Gu et al., 2014). Pathologically, the ALI-induced changes are protein-rich fluids accretion in the alveolar cavities, increased permeability of the alveolocapillary membrane, and inflammatory chemokine production for the influx of neutrophils from blood (Wang et al., 2019). Another work has shown that the pathogenesis of septic ALI involves inflammatory cells activation, with macrophages playing vital roles in immune response *via* cytokines and chemokines release (Lomas-Neira et al., 2006). As part of the innate immune system, inflammasomes are large cytosolic multiprotein complexes that are assembled in response to stimuli such as infection and stress with the capability of regulating caspase 1 activation, which mediates inflammatory responses (de Zoete et al., 2014). On the other hand, available evidence has indicated that inflammation without pathogens (sterile inflammation) is mediated through inflammasomes (Ding et al., 2016). The activation of the best characterized nucleotide-binding oligomerization domain-like receptor protein 3 (NLRP3) inflammasome is *via* cellular stress, which may trigger the innate immune defense system. In recent times, the activation of NLRP3 inflammasome has been implicated in the pathogenesis of various diseases. Putatively, several underlying mechanisms of NLRP3 inflammasome activation have been established with an increased production of reactive oxygen species (ROS) widely accepted as a general sensor for alterations in oxidative stress in cells (Tschopp and Schroder, 2010; Abais et al., 2013). Overproduction of ROS has been shown to cause inflammation and damage to the architecture of lung tissues (Blanco-Ayala et al., 2014). Existing literature has posited that paraquat-induced secretion of cytokines (interleukin-IL-1 $\beta$  and IL-18) coupled with activation of NLRP3 inflammasome was evident in macrophages and ALI animal model (Liu et al., 2015). Besides, aldosterone-induced renal tubular injury through activation of NLRP3 inflammasome was mediated by mitochondrial ROS (Ding et al., 2016). Some treatment options for sepsis-induced ALI have been explored, albeit the unmet need to identify safer and more effective drugs that may target mitochondrial ROS-mediated activation of NLRP3 inflammasome.

Although numerous clinical trials have been undertaken, there is no effective drug to provide outstanding outcomes in preventing sepsis-induced ALI (Chen T. et al., 2020). Drugs including dexamethasone, ulinastatin, prednisone, and prednisolone used for clinical treatment of ALI may result in patients with more severe gastrointestinal irritation, allergy, and other side effects (He et al., 2021). Natural products are one of the main sources of drugs or important lead compounds for the treatment of ALI, with the characteristics of few side effects and low toxicity, strong therapeutic efficacy, and multiple targets

(Ding et al., 2020). As a well-known immunomodulatory Chinese herbal medicine, Radix Astragali (RA, also called astragalus and Huangqi in Chinese) is developed from the dried root of *Astragalus membranaceus* (Chen Z. et al., 2020). It has been widely explored in the traditional Chinese medicine (TCM) practice for the treatment of various inflammation-induced diseases for decades (Auyeung et al., 2016). *Astragalus membranaceus* comprises various constituents such as calycosin (CA), polysaccharides, other flavonoids, saponins, and astragalosides (Gao et al., 2014). However, CA is the most potent component in the dry root of RA. Several works have enumerated the health-promoting effects of CA. Among these, diabetes-induced renal inflammation was ameliorated by CA *via* downregulation of I $\kappa$ B $\alpha$  and nuclear factor- $\kappa$ B (NF- $\kappa$ B) p65 phosphorylation (Zhang et al., 2019). Also, CA was reported to attenuate inflammation in 1-methyl-4-phenyl-1,2,3,6-tetrahydropyridine (MPTP)-induced Parkinson’s disease mice through inhibition of the toll-like receptor (TLR)/NF- $\kappa$ B and MAPK pathways (Yang J. et al., 2019). In another work, oxidative stress and inflammatory response in cerulein-induced acute pancreatitis were inhibited by CA through NF- $\kappa$ B and p38 MAPK signaling pathways (Ma et al., 2018). Despite these promising pharmacological activities of CA, its effect on sepsis-induced ALI has not been fully investigated.

In the present study, we examined the protective role of CA in sepsis-induced ALI *in vitro* and *in vivo*. Putatively, it was proposed that CA may ameliorate lipopolysaccharide (LPS) and cecal ligation and puncture (CLP)-induced lung inflammation *via* the inhibition of mitochondrial ROS-mediated inflammasome activation.

## MATERIALS AND METHOD

### Animal and Approval

Animal experiments in this study were done in the Laboratory Animal Research Center of Jiangsu University. The entire animal research protocols for the experiment were performed based on the guidelines issued by the Institutional Animal Care and Use Committees of Jiangsu University. The ethical approval number is UJS-IACUC-2019042101. Male C57BL/6 mice (6 to 8 weeks old) were purchased from Charles River Laboratories (Beijing, China) and housed in polypropylene cages at 21  $\pm$  2°C under a 12 h light/dark cycle and with food and water provided *ad libitum*.

### Murine Model and Treatment

The sepsis-induced ALI model was established by CLP as described in a previous study with mild modification (Rittirsch et al., 2009). Briefly, mice were anesthetized with ketamine (100 mg per kg body weight *i. p.*) and xylazine (10 mg per kg body weight *i. p.*) (Rittirsch et al., 2009). A middle abdominal incision was performed and the cecum was exposed, ligated, and punctured through and through with a 20-gauge needle. The ligated cecum was then returned to the peritoneal cavity and the abdomen was closed in two layers. In the sham group, mice underwent exactly the same procedures without performing the ligation and puncture process. CA was purchased

from Sigma-Aldrich Corp (St. Louis, MO, #B9938). Mice were divided into five groups ( $n = 10$ ): 1) Sham, 2) CLP, 3) CLP+12.5 mg kg<sup>-1</sup> CA, 4) CLP+25 mg kg<sup>-1</sup> CA, and 5) CLP+50 mg kg<sup>-1</sup> CA. The ligated mice were treated with CA by gavage at 0 and 6 h after CLP. Mice were sacrificed (after 12 h of CLP administration) and the lung tissues were harvested for further analysis. For the survival rate experiment, the ligated mice were treated with CA by gavage once per day. The mortality of mice was monitored every 24 h for 5 days after CLP in each group.

Moreover, sepsis-induced ALI was established by lipopolysaccharide (LPS, Sigma-Aldrich Corp, St. Louis, MO, #L2630) administration followed by application of oleic acid (OA) (Vettorazzi et al., 2015). OA was prepared as a 4% solution in 0.1% bovine serum albumin (BSA). Mice divided into five groups ( $n = 10$ ) as previously described were injected intraperitoneally (i.p.) with 10 mg kg<sup>-1</sup> LPS (Sigma Chemical Co., St. Louis, MO, L2880) and 30 min later intravenously (i.v.) with 2.6  $\mu$ L g<sup>-1</sup> oleic acid (OA, Sigma Chemical Co., St. Louis, MO, #O1008). Mice were treated with CA by gavage at 0 and 6 h after LPS administration. After LPS administration for 12 h, mice were sacrificed and lung tissues were harvested for further analysis. For the survival rate experiment, the 20 mg kg<sup>-1</sup> LPS-injected mice were treated with CA by gavage once per day. The mortality of mice was monitored every 24 h for 5 days after LPS injection in each group. The CLP or LPS-injected mice for survival study were euthanized when they met moribund criteria for humane endpoints, including hunched posture, dyspnea, and absence of righting reflexes after being laid in a lateral recumbent position.

## Histology and Immunohistochemistry

Lung tissues from mice were fixed with 10% formalin overnight and embedded in paraffin wax. Paraffin blocks were then cut into 5  $\mu$ m slices and stained with hematoxylin and eosin (H&E). An overall histopathological score was assigned as described previously (Sweeney et al., 2011): 0 = no lesion, 1 = minimal lesion (<10% of the area involved), 2 = mild lesion (10–30% area involved), 3 = moderate lesion (30–50% area involved), 4 = marked lesion (50–80% area involved), and 5 = severe lesion (>80% area involved). For F4/80 (Cell Signaling Technology, Danvers, MA, #70076) immunohistochemistry, lung tissue slides were fixed and stained using a SignalStain<sup>®</sup> DAB substrate kit (#8059) according to the manufacturer's instructions.

## Lung Wet to Dry Weight Ratio Analysis

The lower part of the right lung was excised and weighed to obtain the wet weight. Then, the wet lung was dried in an oven at 72°C for 48 h to obtain the dry weight. Lung wet to dry (W/D) weight ratio was calculated to assess the lung edema.

## Analysis of Bronchoalveolar Lavage Fluid

Briefly, mice were sacrificed and the tracheae were exposed. Ice-PBS (1 ml) was injected into the lungs and extracted with a syringe. This step was repeated three times. The collected BALF was centrifuged at 1,000 g for 5 min at 4°C. The supernatant was used to detect the levels of interleukin (IL)-1 $\beta$  and IL-18 by ELISA assay. The cell pellet was suspended in 1 ml, and the total number of cells was determined with a hemocytometer. Then, the cells

**TABLE 1** | Primer sequences.

| Name           | Forward/Reverse | Primer sequence<br>(5' to 3') |
|----------------|-----------------|-------------------------------|
| IL-1 $\beta$   | F               | TCC TGT GTA ATG AAA GAC GGC   |
| —              | R               | ACT CCA CTT TGC TCT TGA CTT C |
| IL-18          | F               | CTT CGT TGA CAA AAG ACA GCC   |
| —              | R               | CAC AGC CAG TCC TCT TAC TTC   |
| $\beta$ -Actin | F               | CTT CGT TGA CAA AAG ACA GCC   |
| —              | R               | CAC AGC CAG TCC TCT TAC TTC   |

were subjected to Wright–Giemsa staining according to the manufacturer's instruction. The counts of different cells, including macrophages, lymphocytes, and neutrophils, were viewed and determined with a bright-field microscope.

## Measurement of Biochemical Markers in Lung Tissue

In brief, lung tissue was homogenized in ice-PBS and the supernatants were harvested after centrifugation. The levels of malondialdehyde (MDA, #A003-1-1), superoxide dismutase (SOD, #A001-1-1), glutathione (GSH, #A006-2-1), and myeloperoxidase (MPO, #A004-1-1) in lung tissues were measured using commercial kits (Nanjing Jiancheng Bioengineering Institute, Nanjing, China) in accordance with the manufacturer's protocol.

## Bone Marrow-Derived Macrophages Differentiation and Stimulation

Bone marrow cells were obtained by flushing the femurs and tibias from 6–8 weeks old mice and cultured in Dulbecco's modified Eagle medium containing 50 ng/ml recombinant macrophage-colony stimulating factor (M-CSF, Peprotech, Cranbury, NJ, #315-02), 10% fetal bovine serum (Gibco, Grand Island, NY), penicillin (100 U/ml), and streptomycin (100  $\mu$ g/ml) under a humidified 5% (v/v) CO<sub>2</sub> atmosphere at 37°C for 7 days to form macrophages. BMDMs were treated with 100 ng/ml LPS and 5 mM ATP to activate the inflammasomes.

## RNA Extraction and Real-Time PCR

Lung tissue was homogenized in TRIzol<sup>™</sup> reagent (Invitrogen, Carlsbad, CA) and total RNA was extracted according to the manufacturer's instructions. Total RNA from lung tissue was reverse-transcribed using a RETROscript<sup>®</sup> reverse transcription kit (Invitrogen, Carlsbad, CA, #AM1710). Next, real-time PCR was carried out using cDNA, primers, and SYBR Green Master Mix (Invitrogen, Carlsbad, CA) with an ABI Prism 7500 sequence detection system (Applied Biosystems, Foster City, CA) following the manufacturer's instructions. Amplification of  $\beta$ -actin was used as an internal control. The primers used are summarized in **Table 1**.

## ELISA Assay

Cell culture medium and the BALF samples were harvested after the stimulation or surgical procedures. Measurement of IL-1 $\beta$

(#MLB00C) or IL-18 (#7625) concentration was determined by ELISA kits (R&D Systems, Inc., Minneapolis, MN) according to the manufacturer's instruction.

## Western Blot and Co-Immunoprecipitation Assay

Briefly, the protein was extracted from lung tissue and BMDMs with RIPA lysis buffer containing protease inhibitor cocktail (Cell Signaling Technology, Danvers, MA). The protein concentration was determined by a Pierce™ Bicinchoninic acid (BCA) protein assay kit (Pierce, Rochford, IL, #23227) according to the manufacturer's instructions. An equal amount of denatured protein was loaded to SDS-PAGE gel, separated, and subsequently electro-transferred onto a polyvinylidene fluoride membrane. The membrane was blocked with 5% non-fat milk, incubated with the primary and the horseradish peroxidase-conjugated secondary antibodies (Cell Signaling Technology, Danvers, MA). Blots were visualized using Chemiluminescent Substrate. ImageJ software was used for densitometric analysis. Densitometric values were normalized to  $\beta$ -actin. Mouse reactive inflammasome antibody sampler kit (#20836) purchased from Cell Signaling Technology (Danvers, MA) was used as primary antibody. For co-immunoprecipitation assay, the lysates were immunoprecipitated with NLRP3 antibody or IgG control antibody with protein A/G beads. After washing the beads, the protein bands were visualized by western blot analysis.

## Flow Cytometric Analysis

To evaluate the intracellular ROS production, the treated cells were harvested and incubated with 10  $\mu$ M 2,7-dichlorofluorescein diacetate (DCFH-DA, Sigma-Aldrich Corp, St. Louis, MO, #D6883) at 37°C for 20 min during darkness prior to washing with ice-PBS twice. The DCF fluorescence distribution of  $1 \times 10^4$  events was detected by a FACScan flow cytometry at an excitation wavelength of 488 nm and an emission wavelength of 525 nm. For dihydroethidium (DHE) staining, the treated cells were harvested and incubated with 5  $\mu$ M DHE (Beyotime Biotechnology, Shanghai, China, S0063) at 37°C for 30 min during darkness prior to washing with ice-PBS twice. The DHE fluorescence distribution of  $1 \times 10^4$  events was detected by a FACScan flow cytometry at an excitation wavelength of 370 nm and an emission wavelength of 610 nm. To evaluate superoxide production by mitochondria, the treated cells were harvested and incubated with a 10  $\mu$ M MitoSOX™ Red reagent (2.5  $\mu$ M, Invitrogen, Carlsbad, CA, #M36008) at 37°C for 30 min in the dark before washing with warm buffer twice. The MitoSOX fluorescence distribution of  $1 \times 10^4$  events was detected by a FACScan flow cytometry at an excitation wavelength of 488 nm and an emission wavelength of 620 nm. Fluorescent signal intensity was analyzed with the percentage of subpopulations by FlowJo software.

## Caspase 1 Activity Assay

Caspase 1 activity was measured by a colorimetric assay according to the manufacturer's instruction (Beyotime Biotechnology, Shanghai, China, #C1101). Briefly, the protein was extracted from lung tissues and BMDMs with lysis buffer. The protein concentration was determined by a BCA protein

assay kit (Pierce, Rochford, IL, #23227). Protein (100  $\mu$ g) was incubated with the substrate of caspase 1 (Ac-YVAD-pNA, 10  $\mu$ L, 2 mmol/L) at 37°C for 2 h. The absorbance values of pNA at 405 nm were determined by a spectrophotometer. A standard curve of pNA was performed to calculate the caspase 1 activity.

## Statistical Analysis

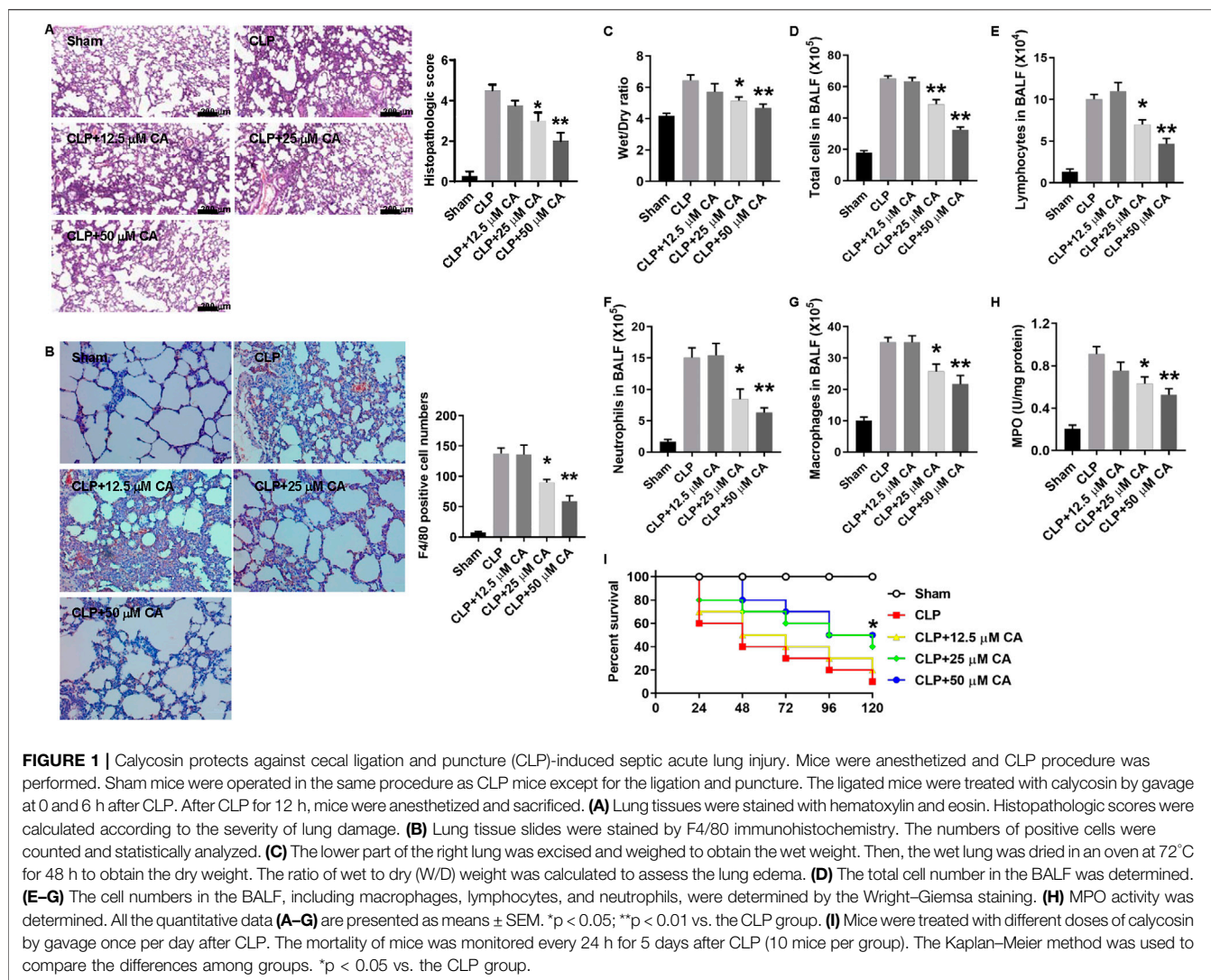
Means  $\pm$  standard error of the mean (SEM) was used to express the data. Statistical analysis was performed by one-way analysis of variance (ANOVA) followed by Dunnett's multiple comparison test using GraphPad Prism 7 software. The Kaplan–Meier method was used to compare the mortality differences among groups. A  $p < 0.05$  was considered statistically significant.

## RESULTS

### Calycosin Protects Against Sepsis-Induced ALI

To evaluate the potential protective effects of CA against sepsis-induced ALI, we used two different murine sepsis models. In the CLP or LPS/OA-injection model, mice were treated with different doses of CA at 0 and 6 h. Within 12 h, none of the mice died in these two models. After CLP or LPS injection for 12 h, lung tissues from mice were collected and H&E staining was used to evaluate the damage of the lung. As shown in **Figure 1A**, the ligated mice have a heavy infiltration of inflammatory cells, exudative changes in the peribronchial layer of the bronchi, edema, and fibrin deposition, while they are attenuated by CA treatment ( $p < 0.05$ , CLP+20;  $p < 0.01$ , CLP+50) and the histopathologic score was significantly decreased. Moreover, F4/80 immunohistochemistry results showed that CA treatment inhibited macrophage infiltration in lung tissue. The number of F4/80 positive cells was significantly decreased in CA-treated mice compared with the no-treatment group (**Figure 1B**). The W/D ratio of lung tissues, which signifies pulmonary edema, was significantly decreased in CA-treated groups compared to the CLP group (**Figure 1C**). Total cell numbers including macrophages, lymphocytes, and neutrophils and MPO activity markedly decreased in CA-treated groups compared with the CLP group (**Figures 1E–H**). Interestingly, the survival rate of mice in the CA-treated groups was significantly improved compared with the CLP group (**Figure 1I**).

**Figure 2** shows the potential beneficial effect of CA on LPS-induced septic ALI. Through H&E staining, it was observed that the sectioned lung tissue of mice in the normal group showed no abnormal changes with normal structural alveolar (**Figure 2A**, Normal), while that of LPS-treated mice (**Figure 2A**, LPS) was pathologically altered and diffused *via* the formation of edema in the interstice, apparent infiltration of inflammatory cells, and structural disarray of alveolar and hemorrhage. Nonetheless, CA treatment improved the histopathologic changes with a substantial ( $p < 0.05$ , LPS+20;  $p < 0.01$ , LPS+50) decrease in the score compared with the LPS group. Consistent with the results of **Figure 1B**, the number of F4/80 positive cells was also significantly decreased in CA-treated mice compared with the no-treatment group (**Figure 2B**). Moreover, the W/D ratio in lung tissue was significantly reduced by CA treatment ( $p < 0.05$ ,



LPS+20;  $p < 0.01$ , LPS+50) compared with the LPS group (Figure 2C). Besides, an obvious ( $p < 0.01$ ) decrease in total cell number in BALF of mice treated with CA was observed compared with that of the LPS group (Figures 2D–G). In addition, CA substantially ( $p < 0.05$ ) improved the survival of the mice after the LPS challenge (Figure 2I). Overall, these results suggest that CA may dose-dependently protect the mice against CLP and LPS-induced septic ALI.

## Calycosin Reduces IL-1 $\beta$ and IL-18 mRNA and Protein Levels in Lung Tissue and BALF

After establishing the two models, real-time PCR and ELISA assay were used to determine IL-1 $\beta$  and IL-18 mRNA and protein levels in lung tissue and BALF. As depicted in Figure 3, the IL-1 $\beta$  and IL-18 mRNA and protein levels increased after CLP and LPS injection. However, administration of CA significantly reduced the production of IL-1 $\beta$  ( $p < 0.05$ , 25 mg kg $^{-1}$ ;  $p < 0.01$ , 50 mg kg $^{-1}$ ) and IL-18 ( $p < 0.01$ ) mRNA level in lung tissue compared with CLP group (Figure 3A). Likewise, protein levels of IL-1 $\beta$  and IL-18 ( $p < 0.05$ ,

25 mg kg $^{-1}$ ;  $p < 0.01$ , 50 mg kg $^{-1}$ ) in the BALF of CA-treated mice decreased obviously compared to those in the CLP group (Figure 3B). In the LPS model, IL-1 $\beta$  and IL-18 levels ( $p < 0.05$ , 25 mg kg $^{-1}$ ;  $p < 0.01$ , 50 mg kg $^{-1}$ ) were substantially reduced in lung tissues of mice treated with CA (Figure 3C). At the protein level, synthesis of IL-1 $\beta$  and IL-18 ( $p < 0.05$ , 25 and  $p < 0.01$ , 50 mg kg $^{-1}$ ) markedly diminished in BALF of CA-treated mice (Figure 3D). Altogether, CA (in a dose-dependent fashion) showed anti-inflammatory effects *via* reducing IL-1 $\beta$  and IL-18 levels in lung tissue and BALF of CA-treated mice.

## Calycosin Inhibits NLRP3 Inflammasome Activation in Lung Tissue

NLRP3 inflammasome activation triggers caspase 1 activation and IL-1 $\beta$  maturation (Yang Y. et al., 2019). The mechanism of anti-inflammatory effect of CA was evaluated by detecting NLRP3 inflammasome activation in lung tissue of mice with sepsis-induced ALI after 12 h *via* western blot analysis. As displayed in Figure 4, the cleaved caspase 1 protein levels generally increased upon CLP or LPS challenge. However, CLP (Figure 4A) and LPS-induced

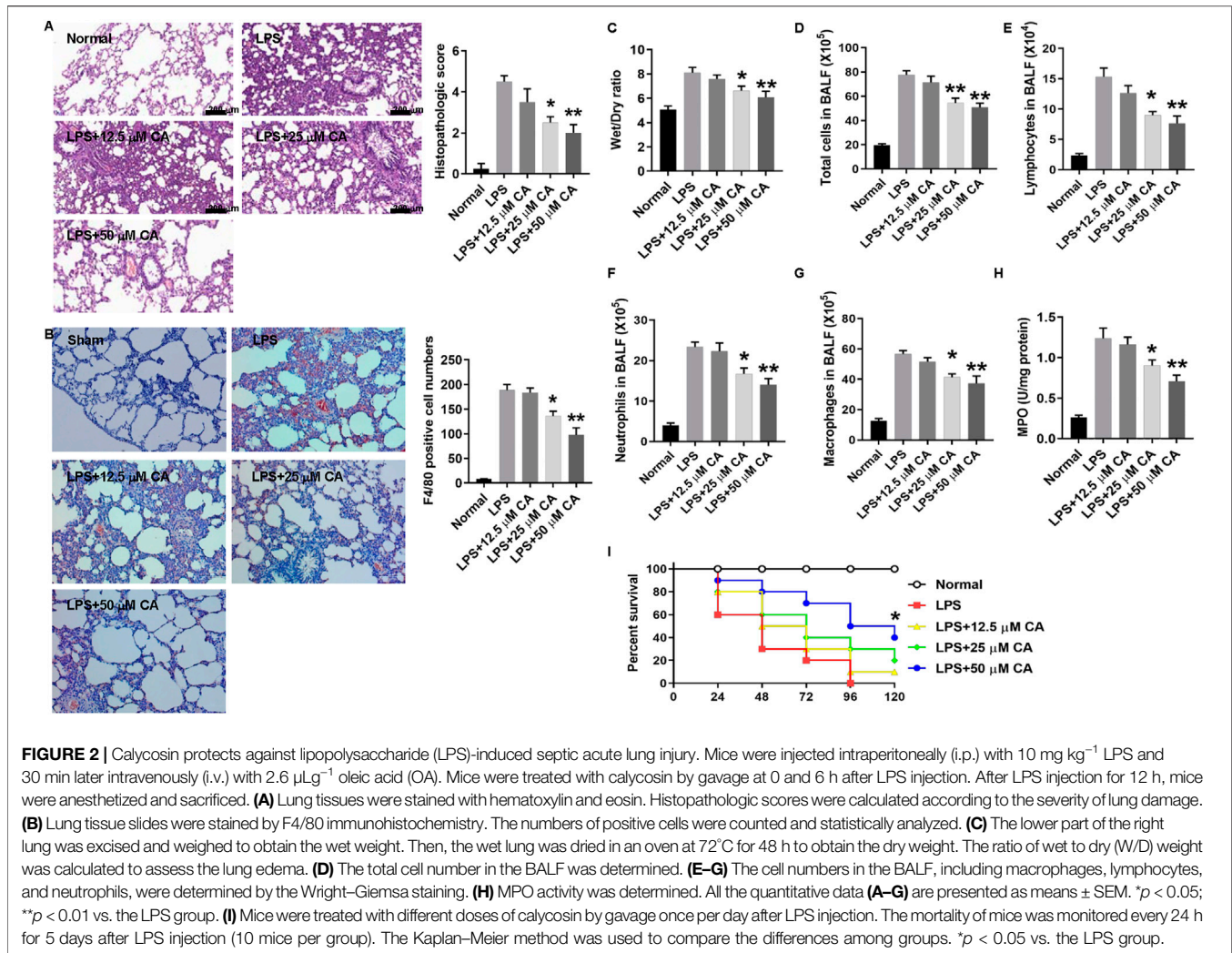


(Figure 4C) high protein levels of cleaved caspase 1 were substantially ( $p < 0.01$ ) suppressed when the mice received CA (50 mg kg<sup>-1</sup>). Contrarily, caspase 1 activity was significantly inhibited by CA treatment compared with CLP ( $p < 0.05$ , CLP+25;  $p < 0.01$ , CLP+50) or LPS ( $p < 0.01$ ) groups (Figures 4B,D). Additionally, as shown in Figures 4A,C, levels of NLRP3 protein did not alter significantly after CA (50 mg kg<sup>-1</sup>) treatment compared with CLP or LPS groups (Figures 4A,C). These data indicated that CA inhibits NLRP3 inflammasome activation in lung tissue.

## Calycosin Suppresses Oxidative Stress in Lung Tissue

To identify the involvement of oxidative stress in CLP or LPS-induced septic ALI, the levels of MDA, SOD and GSH were determined in lung tissue at 12 h. In general, the levels of MDA in lung tissue of CLP or LPS-induced septic ALI mice markedly increased, while that of SOD and GSH decreased (Figure 5). However, when these mice received CA ( $p < 0.05$ -CLP+25,  $p < 0.01$ -CLP+50), the MDA was obviously reduced, while SOD and GSH increased significantly compared with the CLP or LPS group.

Together, these results indicate CA may suppress oxidative stress in lung tissue of sepsis-induced ALI mice by increasing levels of SOD and GSH, while reducing MDA concentration.

## Calycosin Inhibits LPS-Induced NLRP3 Inflammasome Activation in BMDMs.

In order to further ascertain the potential mechanism underlying the anti-inflammatory properties of CA, we determined the activation of NLRP3 inflammasome in BMDMs after 24 h of LPS induction. As shown in Figure 6A, the levels of IL-1β and IL-18 increased obviously in BMDMs after 24 h of LPS+ATP treatment. In comparison with the LPS group, CA (5 and 10 μM) treatment could evidently decrease IL-1β ( $p < 0.01$ ) and IL-18 levels ( $p < 0.05$ , 5 μM;  $p < 0.01$ , 10 μM) in BMDMs. Increased protein levels of cleaved caspase 1 in the LPS+ATP challenge was markedly diminished in BMDMs after CA treatment compared with the LPS group ( $p < 0.01$ , Figure 6B). Meanwhile, the protein levels of NLRP3 in BMDMs of CA-treated mice did not significantly differ from the LPS+ATP group. Co-immunoprecipitation assay results showed that CA at 5 and 10 μM significantly inhibited the

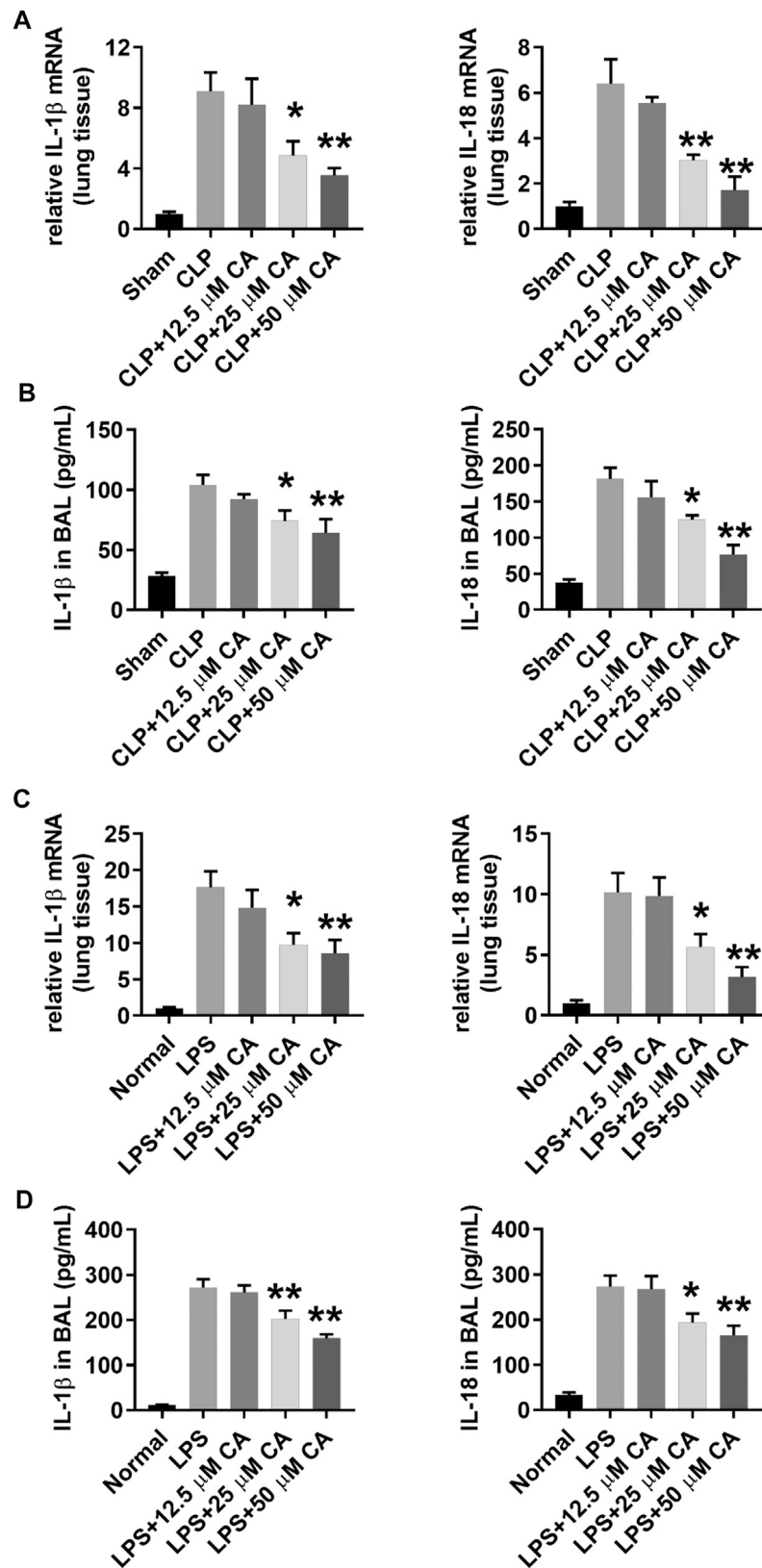


**FIGURE 3** | Calycosin reduces IL-1 $\beta$  and IL-18 mRNA and protein levels in lung tissue and BALF. The ligated or LPS-injected mice were treated with calycosin by gavage at 0 and 6 h. After 12 h, mRNA expression and protein levels in lung tissue and BALF were determined by real-time PCR and ELISA assay (10 mice per group). Data are presented as means  $\pm$  SEM. \* $p$  < 0.05; \*\* $p$  < 0.01 vs. the CLP or LPS group.

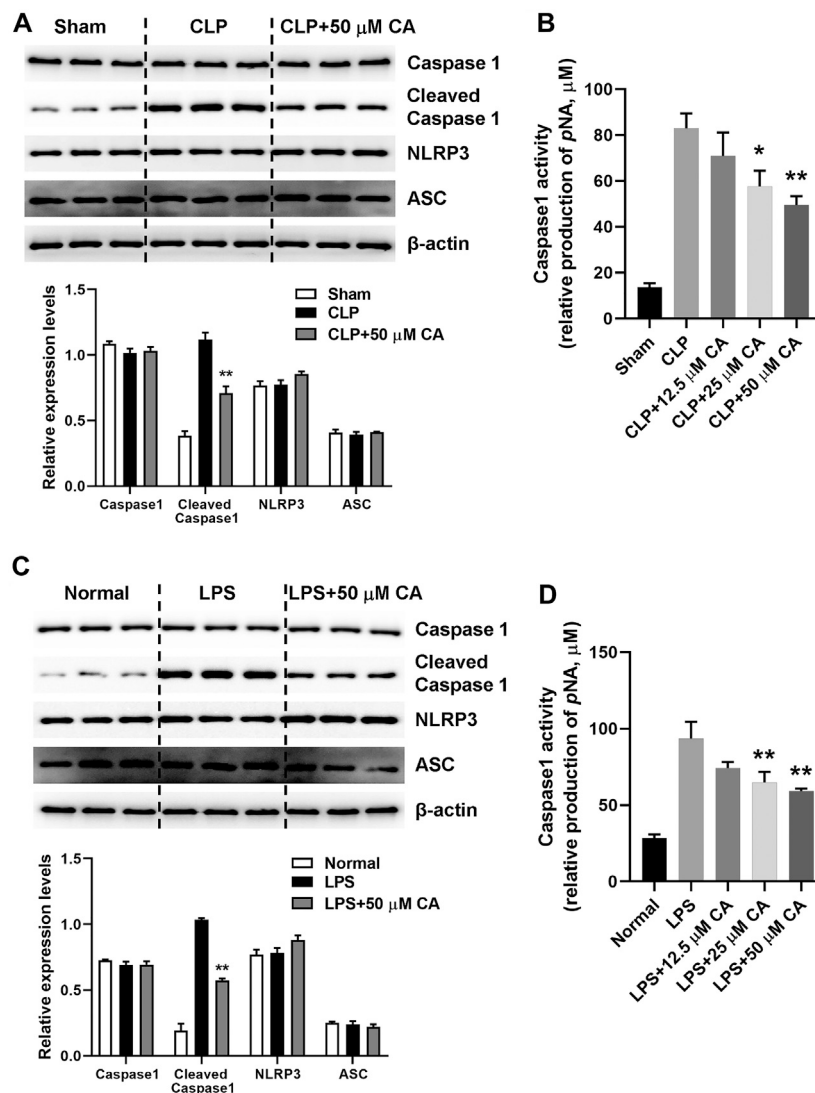


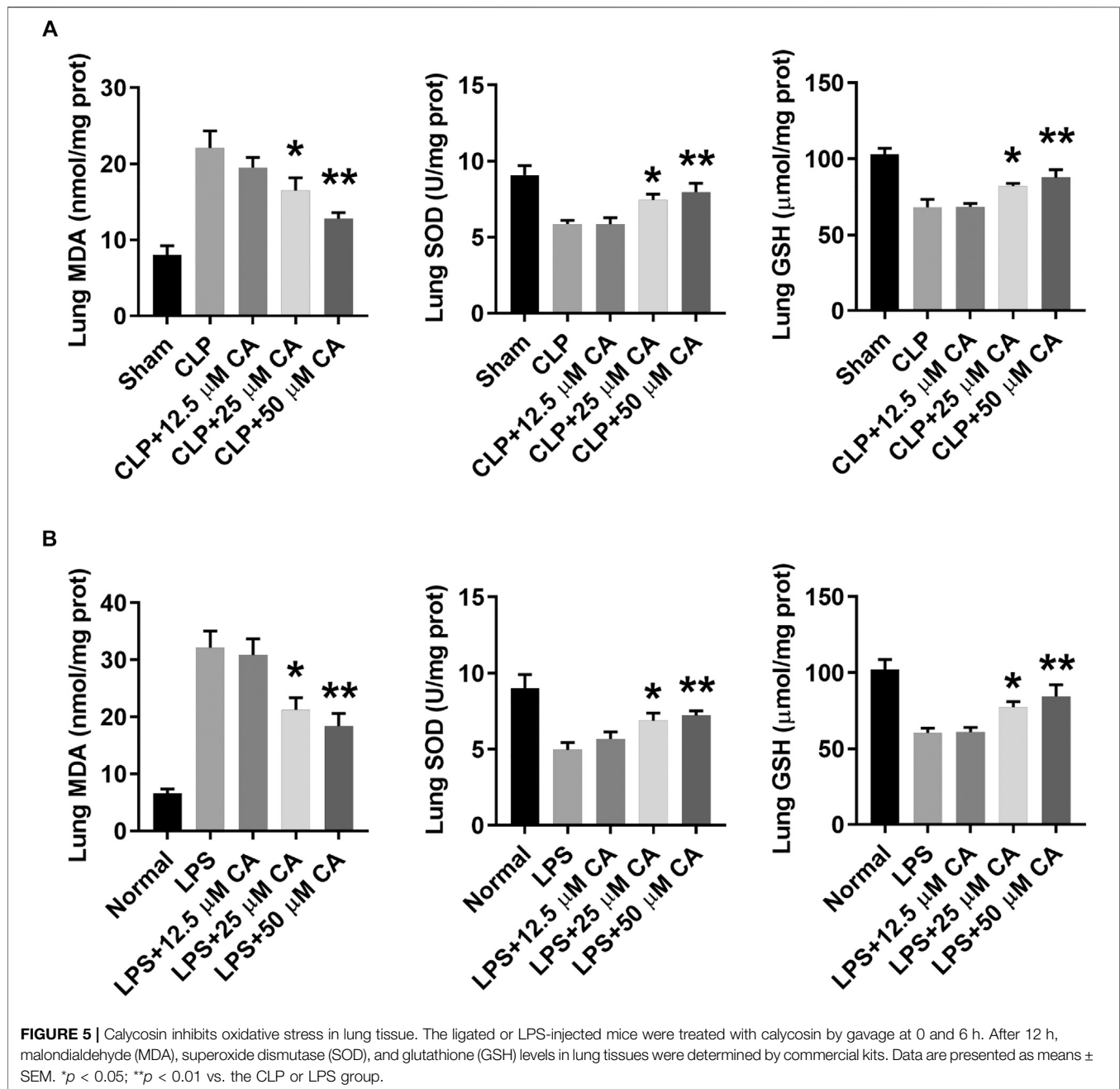
**FIGURE 4** | Calycosin inhibits NLRP3 inflammasome activation in lung tissue. The ligated or LPS-injected mice were treated with calycosin by gavage at 0 and 6 h. After 12 h, NLRP3 inflammasome associated protein levels in lung tissue were determined by western blot analysis. The quantitative densitometry of the protein expressions was determined by Image J software. Densitometric values were normalized to  $\beta$ -actin. The caspase 1 activity in lung tissue was determined by a commercial kit. Data are presented as means  $\pm$  SEM. \* $p < 0.05$ ; \*\* $p < 0.01$  vs. the CLP or LPS group.

interaction among ASC, caspase 1, and NLRP3 in BMDMs (Figure 6C). As displayed in Figure 6D, caspase 1 activity was substantially inhibited by CA compared with that in the LPS group ( $p < 0.01$ ). Overall, CA treatment may inhibit NLRP3 inflammasome activation by decreasing IL-1 $\beta$  and IL-18 levels and suppressing caspase 1 activity.

### Calycosin Reduces LPS-Induced Mitochondrial ROS Production in BMDMs

Through flow cytometric analysis, the underlying mechanism of CA on inhibition of NLRP3 inflammasome activation was

clarified by measuring the production of ROS induced by LPS in BMDMs. In general, the concentration of total ROS in BMDMs increased after LPS stimulation (Figures 7A,B). In contrast, the increased ROS level was evidently decreased after CA treatment in comparison with the LPS group ( $p < 0.01$ ) by DCFH-DA and DHE staining. Next, we detected whether mitochondria were involved in the decrease of CA-induced ROS. MitoSOX<sup>TM</sup> Red was used to measure the level of mitochondrial ROS in CA-treated BMDMs. Compared to the LPS group ( $p < 0.05$ , 5  $\mu$ M;  $p < 0.01$ , 10  $\mu$ M), high levels of mitochondrial ROS were reduced substantially after CA treatment (Figure 7C). Our data indicated that CA could



reduce mitochondrial ROS production in BMDMs in a dose-dependent manner.

### Calycosin Inhibits LPS-Induced NLRP3 Inflammasome Activation by Reducing Mitochondrial ROS Production.

To further understand the mechanism underlying NLRP3 inflammasome activation induced by LPS in CA-treated BMDMs, MitoTEMPO, a mitochondria-targeted superoxide dismutase, was used to measure mitochondrial ROS production in BMDMs. The marked increase in the

concentration of IL-1 $\beta$ , IL-18, cleaved caspase 1 expression, caspase 1 activity, and mitochondrial ROS was observed after the LPS challenge (Figures 8A–D). Compared with the LPS+ATP group, CA (10  $\mu$ M) and MitoTEMPO (10  $\mu$ M) alone treatment prominently decreased levels of IL-1 $\beta$  and IL-18, the activity of caspase 1, cleaved caspase 1 expression, and mitochondrial ROS in BMDMs. Importantly, the results from the combined effect of CA and MitoTEMPO also showed an obvious decrease in BMDM. However, compared with CA alone treatment, levels of IL-1 $\beta$  and IL-18, the activity of caspase 1, cleaved caspase 1 expression, and mitochondrial ROS did not show a further reduction in the combination treatment group, suggesting that

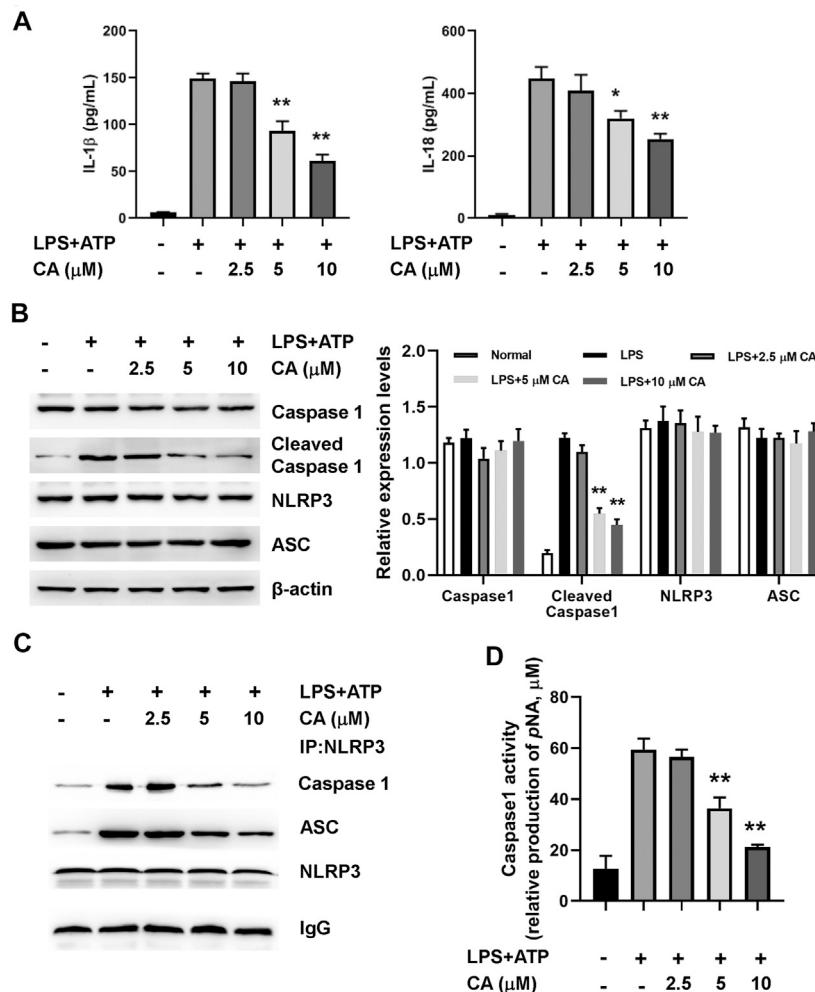


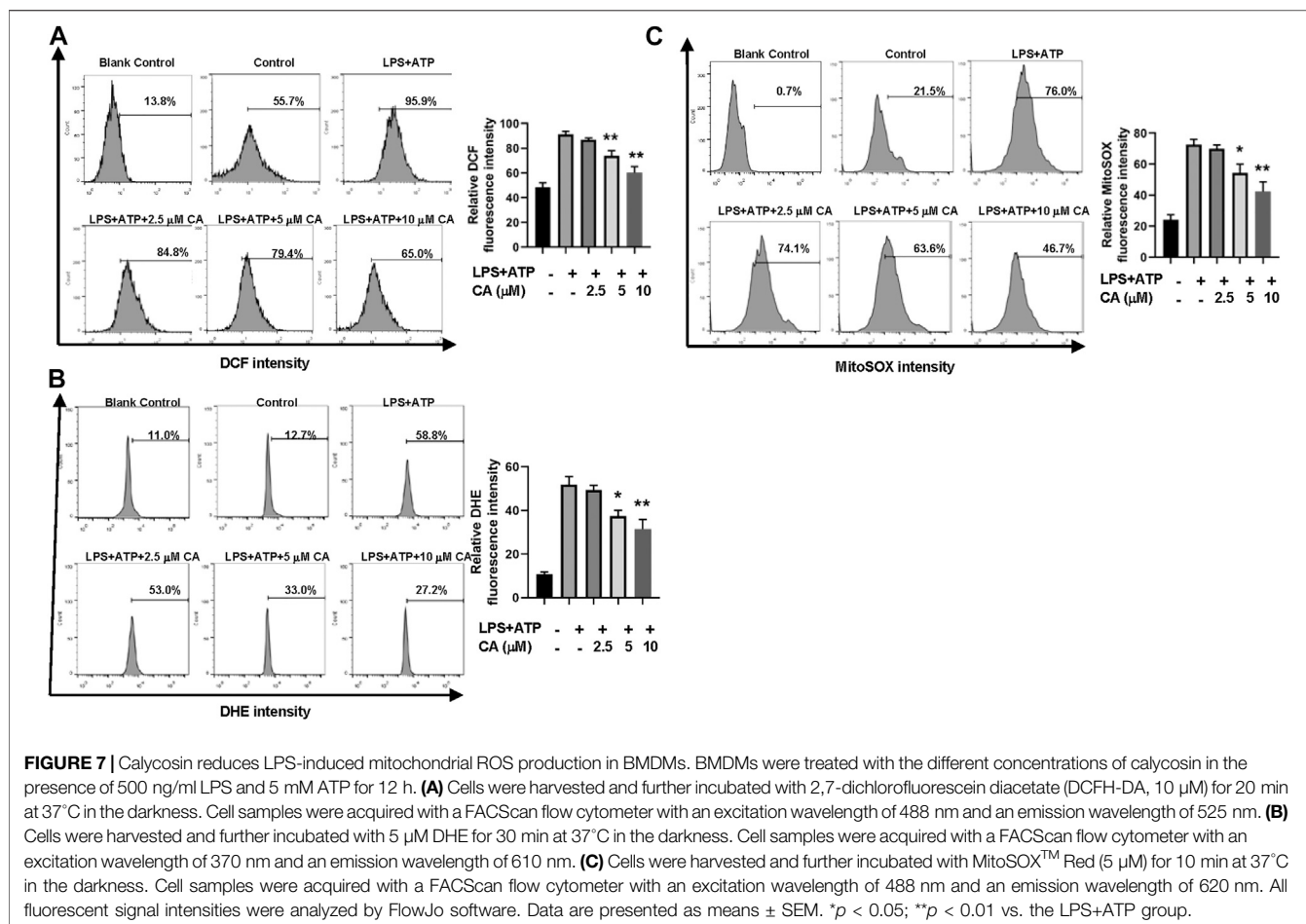
**FIGURE 6** | Calycosin inhibits LPS-induced NLRP3 inflammasome activation in BMDMs. BMDMs cells were treated with the different concentrations of calycosin in the presence of 500 ng/ml LPS and 5 mM ATP for 24 h. **(A)** The levels of IL-1 $\beta$  and IL-18 in the supernatant were determined by ELISA assay. **(B)** The protein levels of NLRP3 inflammasome were determined by western blot. The quantitative densitometry of the protein expressions was determined by Image J software. Densitometric values were normalized to  $\beta$ -actin. **(C)** The effect of CA on the interaction among NLRP3, ASC, and caspase 1 were determined by co-immunoprecipitation assay. **(D)** The caspase 1 activity in BMDMs was determined by a commercial kit. Data are presented as means  $\pm$  SEM. \* $p < 0.05$ ; \*\* $p < 0.01$  vs. the LPS+ATP group.

CA might inhibit mitochondrial ROS-mediated NLRP3 inflammasome activation induced by LPS.

## DISCUSSION

In this study, we indicated that a crucial protective role of CA in sepsis-induced ALI. For the first time, we demonstrated that CA could diminish ALI induced by sepsis by inhibiting inflammasome activation. A cascade of inflammatory mediators released from neutrophils, macrophages, mast cells, and endothelial cells led to the increase of pulmonary microvascular permeability and interstitial and alveolar pulmonary edema in the development of ALI pathogenesis (Herold et al., 2013). Therefore, finding the candidate and elucidating its underlying molecular mechanisms associated

with inflammation may be useful in treating ALI. CA, an isoflavonoid, is a major active component of *Astragalus membranaceus*, which has been widely used in the treatment of inflammatory diseases such as diabetes-induced renal inflammation (Zhang et al., 2019), allergic contact dermatitis (Jia et al., 2018), and myocardial infarction (Cheng et al., 2015). However, few reports have revealed the protective effects of CA on sepsis-induced ALI and its potential mechanism. Here, our results have shown that in CLP or LPS-injected mice, CA attenuated sepsis-induced structural damage and inflammatory cell infiltration in lung tissue and reduced lung wet/dry ratio and inflammatory cell infiltration in BALF and MPO activity. Moreover, CA improved the survival of septic mice induced by CLP or LPS. It has been reported that CA rebalances insulin sensitivity and inflammatory response in gestational diabetes mellitus by suppressing ring finger protein 38



(RNF38) expression (Li et al., 2020). CA not only inhibited the toll-like receptor 4-related protein expression but also reduced NF- $\kappa$ B activation atopic dermatitis model (Tao et al., 2017). Our results from CLP or LPS-injected mice showed that CA reduced IL-1 $\beta$  and IL-18 levels, which indicated that inflammasome activation was inhibited by CA. In line with the ELISA assay, **Figure 4** also shows that CA significantly reduced cleaved caspase 1 expression and activity in lung tissues. Although many studies have reported the multiple functions of CA in inflammatory diseases, the effects of CA on inflammasome activation remain unclear. So far, only one study has reported that CA reduced the levels of sirtuin 1 (Sirt1)-NLRP3 and related proteins in doxorubicin-treated cells and mice hearts, suggesting that CA offers the possibility for the treatment of cardiotoxicity through inhibition of inflammasome (Zhai et al., 2020). Our study provides a rationale for CA to inhibit inflammasome activation in the treatment of ALI.

Inflammasomes, including NLRP3 and ASC, assemble and release inflammatory cytokines (e.g., IL-1 $\beta$  and IL-18) in response to tissue damage after pathogen-associated molecular patterns (PAMPs) or danger-associated molecular patterns (DAMPs) were recognized by pattern recognition receptors (PRRs) (Lamkanfi and Dixit, 2014). Herein, we

found that CA significantly decreased cleaved caspase 1 expression but not NLRP3 and ASC. However, our result showed that CA significantly inhibited the interaction among ASC, caspase 1, and NLRP3 in BMDMs. This result indicates that CA inhibits NLRP3 inflammasome activation by blocking the formation of the NLRP3 inflammasome complex, which may contribute to the inhibition of caspase 1 activity. It was known that LPS and ATP are well-characterized stimulators to trigger inflammasome complex formation (Bednash and Mallampalli, 2016). Our *in vitro* results showed that CA inhibited LPS-induced NLRP3 inflammasome activation in BMDMs and decreased IL-1 $\beta$  and IL-18 levels, caspase 1 activity, and cleaved caspase 1 expression. The mechanisms of inflammasome activation are sophisticated as they respond to injury and danger. It has been reported that caspase 11 is required for the secretion of IL-1 $\beta$  and IL-18 in macrophages after stimulation with LPS, which contributes to non-canonical inflammasome activation (Kayagaki et al., 2011), while the roles of CA in non-canonical inflammasome activation remain incompletely understood.

NLRP3 inflammasome activation is triggered by extracellular ATP existence, intracellular excessive ROS production, potassium efflux, calcium unbalance, and lysosome disruption (Meyers and

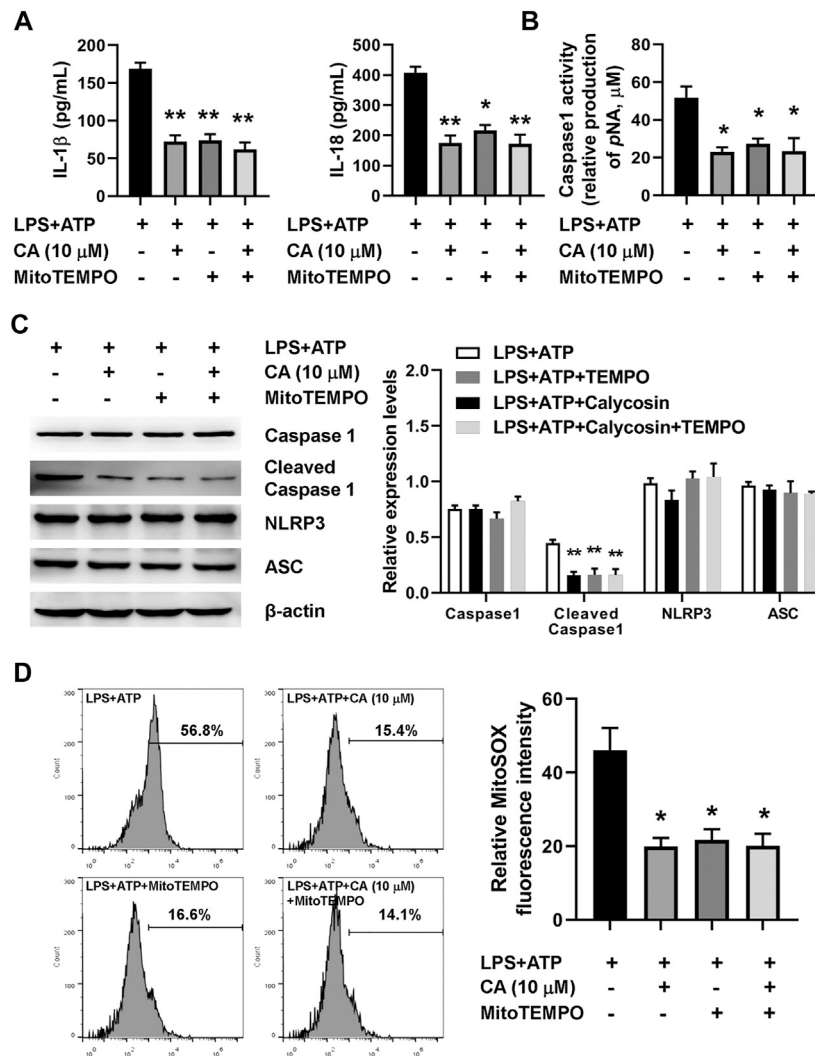


**FIGURE 8** | Calycosin inhibits LPS-induced NLRP3 inflammasome activation through reducing mitochondrial ROS production in BMDMs. The LPS+ATP-induced BMDMs were treated with calycosin (10  $\mu$ M) in the absence or presence of MitoTEMPO (10  $\mu$ M) for 24 h. **(A)** The levels of IL-1 $\beta$  and IL-18 in the supernatant were determined by ELISA assay. **(B)** The caspase 1 activity in BMDMs was determined by a commercial kit. **(C)** The protein levels of NLRP3 inflammasome were determined by western blot. The quantitative densitometry of the protein expressions was determined by Image J software. Densitometric values were normalized to  $\beta$ -actin. **(D)** The LPS+ATP-induced BMDMs were treated with calycosin (10  $\mu$ M) in the absence or presence of MitoTEMPO (10  $\mu$ M) for 12 h. Cells were harvested and further incubated with MitoSOX<sup>TM</sup> Red (5  $\mu$ M) for 10 min at 37°C in the darkness. Cell samples were acquired with a FACScan flow cytometer (Becton Dickinson, United States) with an excitation wavelength of 620 nm and an emission wavelength of 580 nm. Fluorescent signal intensity was analyzed by FlowJo software. Data are presented as means  $\pm$  SEM. \* $p$  < 0.05; \*\* $p$  < 0.01 vs. the LPS+ATP group.

Zhu, 2020). It was well known that abnormal ROS production may cause oxidative stress and subsequent tissue damage (Mullen et al., 2020). Numerous studies have reported that LPS administration increased the levels of ROS and reactive nitrogen species (RNS), which lead to NLRP3 inflammasome activation (Banoth and Cassel, 2018). Toll-like receptor (TLR) 4 activated by LPS drives tumor necrosis factor receptor-associated factor 6 (TRAF6) to translocate to mitochondria, resulting in enhancement of mitochondrial ROS production (Carneiro et al., 2018). CA is an important active isoflavone compound from *Radix Astragali* with a phenolic hydroxyl

group. The phenolic hydroxyl groups on isoflavone can react with free radicals to terminate the chain reaction of free radicals. CA exhibits the protective effect through attenuating oxidative stress in a variety of diseases, including cardiotoxicity (Zhai et al., 2020), Alzheimer's disease (Song et al., 2017), diabetes (Wang and Zhao, 2016), and ischemia-reperfusion injury (Ren et al., 2016). Consistent with these reports, our results showed that CA significantly attenuated oxidative stress in lung tissue and reduced mitochondrial ROS levels markedly in BMDMs. However, our results showed that CA did not alter NLRP3 and ASC expression, indicating that CA with phenolic hydroxyl

group did not inhibit inflammasome activation through changing gene expression. Meanwhile, many studies have reported that CA downregulates NF- $\kappa$ B activity (Yang J. et al., 2019; Zhang et al., 2019). It is predictable that CA not only scavenges ROS but also inhibits NF- $\kappa$ B activity. It is well known that ROS increases NF- $\kappa$ B activity (Sun, 2017). One possible mechanism is that CA decreases NF- $\kappa$ B activity by reducing the level of ROS, which in turn inhibits IL-1 $\beta$  expression. However, few reports have shown the effect of CA on the relationship between ROS and inflammasome activation. Here, we used the mitochondria-targeted antioxidant to prove that mitochondrial ROS attenuated by CA contributes to inflammasome inactivation in macrophages, suggesting that mitochondria probably serve as a target for the treatment of ALI by CA.

In summary, this study has revealed the potential protective effect of CA as an anti-inflammatory candidate to counteract the inflammatory state *in vivo* and *in vitro*. Our data strongly suggest that the advantage of CA in the treatment of sepsis is the reversal of lung injury and the inhibition of excessive inflammasome activation. Moreover, the unique role of CA in reducing mitochondrial ROS in macrophages offers the possibility of a new therapeutic strategy for the treatment of sepsis. Further studies in clinical trials may provide more insight into the functional roles of CA in the treatment of ALI.

## REFERENCES

- Abais, J. M., Zhang, C., Xia, M., Liu, Q., Gehr, T. W., Boini, K. M., et al. (2013). NADPH Oxidase-Mediated Triggering of Inflammasome Activation in Mouse Podocytes and Glomeruli during Hyperhomocysteinemia. *Antioxid. Redox Signal.* 18 (13), 1537–1548. doi:10.1089/ars.2012.4666
- Auyeung, K. K., Han, Q. B., and Ko, J. K. (2016). Astragalus Membranaceus: A Review of its Protection against Inflammation and Gastrointestinal Cancers. *Am. J. Chin. Med.* 44 (1), 1–22. doi:10.1142/s0192415x16500014
- Aziz, M., Jacob, A., Yang, W. L., Matsuda, A., and Wang, P. (2013). Current Trends in Inflammatory and Immunomodulatory Mediators in Sepsis. *J. Leukoc. Biol.* 93 (3), 329–342. doi:10.1189/jlb.0912437
- Aziz, M., Ode, Y., Zhou, M., Ochani, M., Holodick, N. E., Rothstein, T. L., et al. (2018). B-1a Cells Protect Mice from Sepsis-Induced Acute Lung Injury. *Mol. Med.* 24 (1), 26. doi:10.1186/s10020-018-0029-2
- Banoth, B., and Cassel, S. L. (2018). Mitochondria in Innate Immune Signaling. *Transl. Res.* 202, 52–68. doi:10.1016/j.trsl.2018.07.014
- Bednash, J. S., and Mallampalli, R. K. (2016). Regulation of Inflammasomes by Ubiquitination. *Cell Mol Immunol* 13 (6), 722–728. doi:10.1038/cmi.2016.15
- Blanco-Ayala, T., Andérica-Romero, A. C., and Pedraza-Chaverri, J. (2014). New Insights into Antioxidant Strategies against Paraquat Toxicity. *Free Radic. Res.* 48 (6), 623–640. doi:10.3109/10715762.2014.899694
- Carneiro, F. R. G., Lepelley, A., Seeley, J. J., Hayden, M. S., and Ghosh, S. (2018). An Essential Role for ECSIT in Mitochondrial Complex I Assembly and Mitophagy in Macrophages. *Cell Rep* 22 (10), 2654–2666. doi:10.1016/j.celrep.2018.02.051
- Chen, T., Zhu, G., Meng, X., and Zhang, X. (2020a). Recent Developments of Small Molecules with Anti-inflammatory Activities for the Treatment of Acute Lung Injury. *Eur. J. Med. Chem.* 207, 112660. doi:10.1016/j.ejmech.2020.112660
- Chen, Z., Liu, L., Gao, C., Chen, W., Vong, C. T., Yao, P., et al. (2020b). Astragali Radix (Huangqi): A Promising Edible Immunomodulatory Herbal Medicine. *J. Ethnopharmacol* 258, 112895. doi:10.1016/j.jep.2020.112895
- Cheng, Y., Zhao, J., Tse, H. F., Le, X. C., and Rong, J. (2015). Plant Natural Products Calycosin and Gallic Acid Synergistically Attenuate Neutrophil Infiltration and

## DATA AVAILABILITY STATEMENT

The raw data supporting the conclusion of this article will be made available by the authors without undue reservation.

## ETHICS STATEMENT

The animal study was reviewed and approved by the Institutional Animal Care and Use Committees of Jiangsu University.

## AUTHOR CONTRIBUTIONS

YX, YC, and YS conceived and designed the experiments. YX, YC, YS, XH, YT, JY, HH, WM, KQ, and RB performed the experiments. YX, YC, YS, XH, and YT analyzed the data. JY, HH, WM, KQ, and RB contributed reagents/materials/analysis tools. YX, YC, YS, and XH wrote the paper.

## FUNDING

This work was supported by Medical clinical science and technology development fund of Jiangsu University (JLY2021164).

- Subsequent Injury in Isoproterenol-Induced Myocardial Infarction: A Possible Role for Leukotriene B<sub>4</sub> 12-Hydroxydehydrogenase. *Oxid. Med. Cel Longev* 2015, 434052. doi:10.1155/2015/434052
- de Zoete, M. R., Palm, N. W., Zhu, S., and Flavell, R. A. (2014). Inflammasomes. *Cold Spring Harb Perspect. Biol.* 6 (12), a016287. doi:10.1101/cshperspect.a016287
- Ding, W., Guo, H., Xu, C., Wang, B., Zhang, M., and Ding, F. (2016). Mitochondrial Reactive Oxygen Species-Mediated NLRP3 Inflammasome Activation Contributes to Aldosterone-Induced Renal Tubular Cells Injury. *Oncotarget* 7 (14), 17479–17491. doi:10.18632/oncotarget.8243
- Ding, Z., Zhong, R., Xia, T., Yang, Y., Xing, N., Wang, W., et al. (2020). Advances in Research into the Mechanisms of Chinese Materia Medica against Acute Lung Injury. *Biomed. Pharmacother.* 122, 109706. doi:10.1016/j.biopha.2019.109706
- Gao, J., Liu, Z. J., Chen, T., and Zhao, D. (2014). Pharmaceutical Properties of Calycosin, the Major Bioactive Isoflavonoid in the Dry Root Extract of Radix Astragali. *Pharm. Biol.* 52 (9), 1217–1222. doi:10.3109/13880209.2013.879188
- Gu, W. J., Wan, Y. D., Tie, H. T., Kan, Q. C., and Sun, T. W. (2014). Risk of Acute Lung Injury/acute Respiratory Distress Syndrome in Critically Ill Adult Patients with Pre-existing Diabetes: a Meta-Analysis. *PLoS One* 9 (2), e90426. doi:10.1371/journal.pone.0090426
- He, Y. Q., Zhou, C. C., Yu, L. Y., Wang, L., Deng, J. L., Tao, Y. L., et al. (2021). Natural Product Derived Phytochemicals in Managing Acute Lung Injury by Multiple Mechanisms. *Pharmacol. Res.* 163, 105224. doi:10.1016/j.phrs.2020.105224
- Herold, S., Gabrielli, N. M., and Vadász, I. (2013). Novel Concepts of Acute Lung Injury and Alveolar-Capillary Barrier Dysfunction. *Am. J. Physiol. Lung Cel Mol Physiol* 305 (10), L665–L681. doi:10.1152/ajplung.00232.2013
- Hotchkiss, R. S., and Karl, I. E. (2003). The Pathophysiology and Treatment of Sepsis. *N. Engl. J. Med.* 348 (2), 138–150. doi:10.1056/NEJMra021333
- Jia, Z., Wang, X., Wang, X., Wei, P., Li, L., Wu, P., et al. (2018). Calycosin Alleviates Allergic Contact Dermatitis by Repairing Epithelial Tight Junctions via Down-Regulating HIF-1 $\alpha$ . *J. Cel Mol Med* 22 (9), 4507–4521. doi:10.1111/jcmm.13763
- Kayagaki, N., Warming, S., Lamkanfi, M., Vande Walle, L., Louie, S., Dong, J., et al. (2011). Non-canonical Inflammasome Activation Targets Caspase-11. *Nature* 479 (7371), 117–121. doi:10.1038/nature10558

- Lamkanfi, M., and Dixit, V. M. (2014). Mechanisms and Functions of Inflammasomes. *Cell* 157 (5), 1013–1022. doi:10.1016/j.cell.2014.04.007
- Li, Y., Duan, B., Li, Y., Yu, S., and Wang, Y. (2020). The Isoflavonoid Calycosin Inhibits Inflammation and Enhances Beta Cell Function in Gestational Diabetes Mellitus by Suppressing RNF38 Expression. *Immunopharmacol Immunotoxicol* 42 (4), 366–372. doi:10.1080/08923973.2020.1782426
- Liu, Z., Zhao, H., Liu, W., Li, T., Wang, Y., and Zhao, M. (2015). NLRP3 Inflammasome Activation Is Essential for Paraquat-Induced Acute Lung Injury. *Inflammation* 38 (1), 433–444. doi:10.1007/s10753-014-0048-2
- Lomas-Neira, J., Chung, C. S., Perl, M., Gregory, S., Biffl, W., and Ayala, A. (2006). Role of Alveolar Macrophage and Migrating Neutrophils in Hemorrhage-Induced Priming for ALI Subsequent to Septic challenge. *Am. J. Physiol. Lung Cell Mol Physiol* 290 (1), L51–L58. doi:10.1152/ajplung.00028.2005
- Ma, R., Yuan, F., Wang, S., Liu, Y., Fan, T., and Wang, F. (2018). Calycosin Alleviates Cerulein-Induced Acute Pancreatitis by Inhibiting the Inflammatory Response and Oxidative Stress via the P38 MAPK and NF-Kb Signal Pathways in Mice. *Biomed. Pharmacother.* 105, 599–605. doi:10.1016/j.biopha.2018.05.080
- Meyers, A. K., and Zhu, X. (2020). The NLRP3 Inflammasome: Metabolic Regulation and Contribution to Inflammaging. *Cells* 9 (8). doi:10.3390/cells9081808
- Mullen, L., Mengozzi, M., Hanschmann, E. M., Alberts, B., and Ghezzi, P. (2020). How the Redox State Regulates Immunity. *Free Radic. Biol. Med.* 157, 3–14. doi:10.1016/j.freeradbiomed.2019.12.022
- Ren, M., Wang, X., Du, G., Tian, J., and Liu, Y. (2016). Calycosin-7-O- $\beta$ -D-glucoside Attenuates Ischemia-Reperfusion Injury *In Vivo* via Activation of the PI3K/Akt Pathway. *Mol. Med. Rep.* 13 (1), 633–640. doi:10.3892/mmr.2015.4611
- Rittirsch, D., Huber-Lang, M. S., Flierl, M. A., and Ward, P. A. (2009). Immunodesign of Experimental Sepsis by Cecal Ligation and Puncture. *Nat. Protoc.* 4 (1), 31–36. doi:10.1038/nprot.2008.214
- Sevransky, J. E., Martin, G. S., Shanholtz, C., Mendez-Tellez, P. A., Pronovost, P., Brower, R., et al. (2009). Mortality in Sepsis versus Non-sepsis Induced Acute Lung Injury. *Crit. Care* 13 (5), R150. doi:10.1186/cc8048
- Singer, M., Deutschman, C. S., Seymour, C. W., Shankar-Hari, M., Annane, D., Bauer, M., et al. (2016). The Third International Consensus Definitions for Sepsis and Septic Shock (Sepsis-3). *Jama* 315 (8), 801–810. doi:10.1001/jama.2016.0287
- Song, L., Li, X., Bai, X. X., Gao, J., and Wang, C. Y. (2017). Calycosin Improves Cognitive Function in a Transgenic Mouse Model of Alzheimer's Disease by Activating the Protein Kinase C Pathway. *Neural Regen. Res.* 12 (11), 1870–1876. doi:10.4103/1673-5374.219049
- Sun, S. C. (2017). The Non-canonical NF-Kb Pathway in Immunity and Inflammation. *Nat. Rev. Immunol.* 17 (9), 545–558. doi:10.1038/nri.2017.52
- Sweeney, K. A., Dao, D. N., Goldberg, M. F., Hsu, T., Venkataswamy, M. M., Henao-Tamayo, M., et al. (2011). A Recombinant Mycobacterium Smegmatis Induces Potent Bactericidal Immunity against *Mycobacterium tuberculosis*. *Nat. Med.* 17 (10), 1261–1268. doi:10.1038/nm.2420
- Tao, Y., Wang, Y., Wang, X., Wang, C., Bao, K., Ji, L., et al. (2017). Calycosin Suppresses Epithelial Derived Initiative Key Factors and Maintains Epithelial Barrier in Allergic Inflammation via TLR4 Mediated NF-Kb Pathway. *Cell Physiol Biochem* 44 (3), 1106–1119. doi:10.1159/000485416
- Tschopp, J., and Schroder, K. (2010). NLRP3 Inflammasome Activation: The Convergence of Multiple Signalling Pathways on ROS Production. *Nat. Rev. Immunol.* 10 (3), 210–215. doi:10.1038/nri2725
- Vettorazzi, S., Bode, C., Dejager, L., Frappart, L., Shelest, E., Klaffen, C., et al. (2015). Glucocorticoids Limit Acute Lung Inflammation in Concert with Inflammatory Stimuli by Induction of SphK1. *Nat. Commun.* 6, 7796. doi:10.1038/ncomms8796
- Vincent, J. L., Marshall, J. C., Namendys-Silva, S. A., François, B., Martin-Loeches, I., Lipman, J., et al. (2014). Assessment of the Worldwide burden of Critical Illness: the Intensive Care over Nations (ICON) Audit. *Lancet Respir. Med.* 2 (5), 380–386. doi:10.1016/s2213-2600(14)70061-x
- Wang, J., Gong, S., Wang, F., Niu, M., Wei, G., He, Z., et al. (2019). Granisetron Protects Polymicrobial Sepsis-Induced Acute Lung Injury in Mice. *Biochem. Biophys. Res. Commun.* 508 (4), 1004–1010. doi:10.1016/j.bbrc.2018.12.031
- Wang, X., and Zhao, L. (2016). Calycosin Ameliorates Diabetes-Induced Cognitive Impairments in Rats by Reducing Oxidative Stress via the PI3K/Akt/GSK-3 $\beta$  Signaling Pathway. *Biochem. Biophys. Res. Commun.* 473 (2), 428–434. doi:10.1016/j.bbrc.2016.03.024
- Yang, J., Jia, M., Zhang, X., and Wang, P. (2019a). Calycosin Attenuates MPTP-Induced Parkinson's Disease by Suppressing the Activation of TLR/NF-Kb and MAPK Pathways. *Phytother. Res.* 33 (2), 309–318. doi:10.1002/ptr.6221
- Yang, Y., Wang, H., Kouadir, M., Song, H., and Shi, F. (2019b). Recent Advances in the Mechanisms of NLRP3 Inflammasome Activation and its Inhibitors. *Cell Death Dis* 10 (2), 128. doi:10.1038/s41419-019-1413-8
- Zhai, J., Tao, L., Zhang, S., Gao, H., Zhang, Y., Sun, J., et al. (2020). Calycosin Ameliorates Doxorubicin-Induced Cardiotoxicity by Suppressing Oxidative Stress and Inflammation via the Sirtuin 1-NOD-like Receptor Protein 3 Pathway. *Phytother. Res.* 34 (3), 649–659. doi:10.1002/ptr.6557
- Zhang, Y. Y., Tan, R. Z., Zhang, X. Q., Yu, Y., and Yu, C. (2019). Calycosin Ameliorates Diabetes-Induced Renal Inflammation via the NF-Kb Pathway *In Vitro* and *In Vivo*. *Med. Sci. Monit.* 25, 1671–1678. doi:10.12659/msm.915242

**Conflict of Interest:** The authors declare that the research was conducted in the absence of any commercial or financial relationships that could be construed as a potential conflict of interest.

**Publisher's Note:** All claims expressed in this article are solely those of the authors and do not necessarily represent those of their affiliated organizations, or those of the publisher, the editors and the reviewers. Any product that may be evaluated in this article, or claim that may be made by its manufacturer, is not guaranteed or endorsed by the publisher.

Copyright © 2021 Xia, Cao, Sun, Hong, Tang, Yu, Hu, Ma, Qin and Bao. This is an open-access article distributed under the terms of the Creative Commons Attribution License (CC BY). The use, distribution or reproduction in other forums is permitted, provided the original author(s) and the copyright owner(s) are credited and that the original publication in this journal is cited, in accordance with accepted academic practice. No use, distribution or reproduction is permitted which does not comply with these terms.